On the performance of PVDF based piezoelectric sensor with microstructures

Rishikesh Srinivasaraghavan Govindarajan^a, Taylor Stark^a, Foram Madiyar^b, Daewon Kim*^a

Dept. of Aerospace Engineering; ^bDept. of Physical Science;

Embry-Riddle Aeronautical University, 1 Aerospace Blvd., Daytona Beach, FL, USA 32114

ABSTRACT

This paper aims to investigate the performance of piezoelectric sensors with different shapes of 3D-printed microstructures. Based on the numerical analysis in the time-frequency domain, the microstructures are printed directly on the PVDF transparent film exhibiting higher piezoelectric coefficients using a high-resolution two-photon polymerization method. Bi-directional gold IDTs are fabricated by sputtering gold onto the substrate surface using a 3D-printed stencil. The mechanical properties of the film and surface morphology of printed microstructures are examined using a nanoindenter and a 3D profilometer. The change in frequency response due to the microstructure is measured using a network analyzer. This study will be a reference for developing an efficient wave-based gas sensor with enhanced sensitivity.

Keywords: microstructures, two-photon polymerization, PVDF, sensor

1. INTRODUCTION

The ever increasing demand for a gas-sensing microdevice in the detection of toxic and hazardous environmental gases necessitates the development of a piezoelectric sensor for real-time monitoring applications in the defense and civil sectors^{1, 2}. Surface acoustic wave sensor (SAW) is a microelectromechanical system (MEMS) that utilizes the propagation of acoustic waves to detect the presence and concentration of the analyte. SAW sensors are extensively used for detecting physical quantities such as strain, pressure, and temperature³⁻⁶. Among different gas detection sensors, SAW exhibits excellent response time, small size, low cost, ability to work in wired and wireless mode, and is mainly compatible with modern fabrication technologies. Particularly, the selected sensor type showcases high sensitivity towards surface perturbation, such as molecular adsorption and change in viscoelastic properties that amend the wave characteristics propagating in the piezoelectric substrate as compared to the input signal's parameter.

To date, SAW microdevices are coated with a suitable sensing material, such as metal oxides or metals, to sense the targeted gas effectively⁷⁻⁹. Among different metal oxides, zinc oxide (ZnO) is widely used as a gas sensing material for detecting carbon dioxide (CO₂), ammonia (NH₃), and nitrogen dioxide (NO₂) gases due to its superior physiochemical properties, long-term stability, and quick response time¹⁰⁻¹³. Various thin film deposition techniques have been utilized, including spray pyrolysis, spin coating and vapor deposition. Major mechanical attributes to be considered are the surface area and thickness of the metal oxide layer, as it dictates the adsorption efficiency. Even though these techniques provide a homogenous coating with better sensor performance, attaining a thick volume of sensing material is challenging and expensive. The effort in this research is towards the fabrication of a novel approach by integrating microstructures in the sensing layer, enabling a larger surface area that can be coated with ZnO thin film through vapor deposition techniques. A detailed study of the sensor with microstructure is crucial to ensure elements added to the sensing layer will not degrade its performance. Numerical simulations are performed to examine the change in sensor characteristics, such as resonant frequency and output voltage, in both time and frequency domains with different microstructures.

The conventional methods for fabrication of microstructures in the sensing layer, such as photo structuring, etching, and molding ¹⁴⁻¹⁶, are a monotonous multi-step process that lacks resolution and requires immense processing time. Additive manufacturing (AM) technology has advanced to the point where micro- and nano-scale structures fabrication is feasible with minimized material utilization and reduced mass production costs ^{17, 18}. This research is geared towards a novel sensor

^{*}kimd3c@erau.edu; phone 1-386-226-7262; ERAU SMART lab

development with microstructure printed directly to the piezoelectric substrate using the two-photon polymerization (2PP) principle. This eliminates the need for a laborious molding process, which is the current bottleneck in the field. A suitable combination of the piezoelectric substrate, interdigital transducer (IDT), and microstructure coated with sensing material is essential for a sensitive micro-device development. Polyvinylidene fluoride (PVDF), a well-known polymer for its excellent piezoelectric property, is selected as a substrate material due to its compliance to flexible micro-MEMS device fabrication. Gold electrodes are deposited on the substrate's surface using a 2PP printed stencil with an IDT pattern, which eliminates the clean room requirement. Figure 1 indicates the overall sensor fabrication steps, including microstructure patterning and electrode deposition.

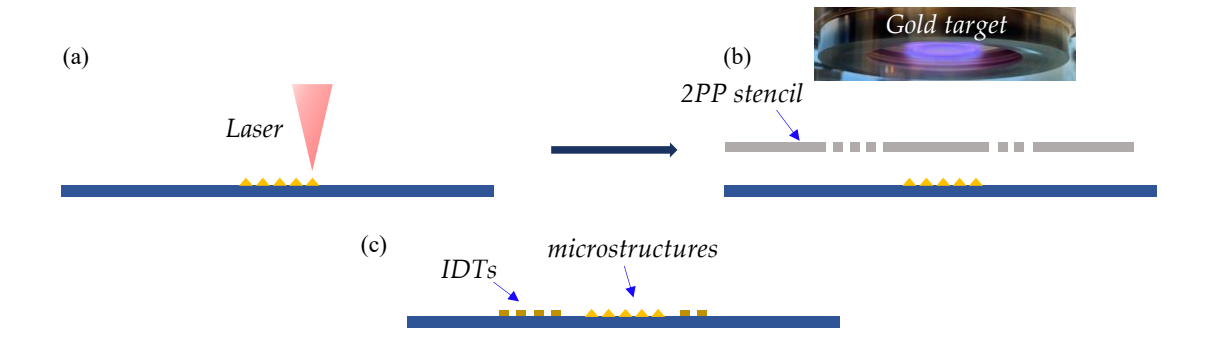


Figure 1. The fabrication process of a piezoelectric sensor with microstructures. (a) 2PP printing of microstructures on PVDF film; (b) electrode deposition using 2PP printed stencil and (c) developed sensor.

2. NUMERICAL ANALYSIS OF SAW WITH MICROSTRUCTURES

2.1 Microstructure designs

Adding microstructures to the sensing layer plays a vital role in sensor performance, as they increase the adsorption rate with an increase in surface area. Different microstructure shapes such as cone, pyramid, dome, and conical frustum, are selected based on their ability to be coated with a metal oxide thin film that enables a sensing mechanism. It is essential to study the influence of microstructure implementation on sensing performance before coating with metal oxides. A microstructure 4x7 grid with $50 \mu m$ height and $100 \mu m$ spacing is selected, increasing the surface area to a maximum of 39.36 %, as listed in Table 1.

Table 1. Microstructure dimensions and surface area enhancement.

Micro-shapes	Dimensions Diameter (µm)	Sensing area with microstructures (µm²)	% Increase in Surface area	(a) cone; (b) pyramid; (c) dome and (d) conical frustum	
Cone	200	3,924,525	27.42		
Pyramid	200	4,292,188	39.36	(a)	(b)
Dome	200	3,928,232	27.54		(d)
Conical frustum	200 (bottom)/ 50 (top)	4,094,692	32.95	(c)	

Finite element modeling allows appropriate optimization of sensor performance with added microstructures conveniently before fabrication, which can be validated using experimental results. In this work, PVDF substrate with added microstructure shapes is simulated numerically using a COMSOL Multiphysics tool^{18, 19}. All the required mechanical and piezoelectric material properties related to the physics used for substrate (PVDF), electrode (gold), and microstructures (acrylic plastic - material similar to Nanoscribe IP-S resin printed during the experiment) are assigned to respective designed domains, as listed in Table 2. A lower reflective boundary at the side walls and a fixed constraint on the bottom

surface are assigned, respectively. Overall domain with PVDF substrate, IDT layouts with microstructures in between are meshed using a tetrahedral element.

Table 2. Material properties of piezoelectric SAW sensor.

Description	Value				
Polyvinylidene fluoride (PVDF)					
Density ρ [kg/m ³]	1,780				
Young's modulus E [GPa]	2				
Poisson's ratio v	0.30				
Elastic compliance matrix [10 ⁻¹⁰ . Pa ⁻¹] Dielectric constant	$s_{11} = 3.78$ $s_{12} = -1.48$ $s_{13} = -1.72$ $s_{33} = 10.92$ $s_{44} = 14.28$ $s_{66} = 11.10$ $\varepsilon_{11} = 7.40$ $\varepsilon_{22} = 9.30$ $\varepsilon_{33} = 7.60$				
Gold (Ag)					
Density ρ [kg/m ³]	19,300				
Young's modulus E [GPa]	70				
Poisson's ratio v	0.44				
Acrylic plastic					
Density ρ [kg/m³]	1,190				
Young's modulus E [GPa]	3.2				
Poisson's ratio v	0.35				

2.2 Frequency domain study

A frequency domain analysis is studied to simulate microstructures' effect on scattering parameter $[S_{21}]$, which dictates the performance of resonant frequency represented in dB with reference 50 Ω impedance. The distinct response received for each microstructure design is obtained from the output IDT in the transmission line, as shown in Figure 2 (a) and (b). A minimal change in resonant peak with a change in loss intensity can be noticed, which is validated with VNA response.

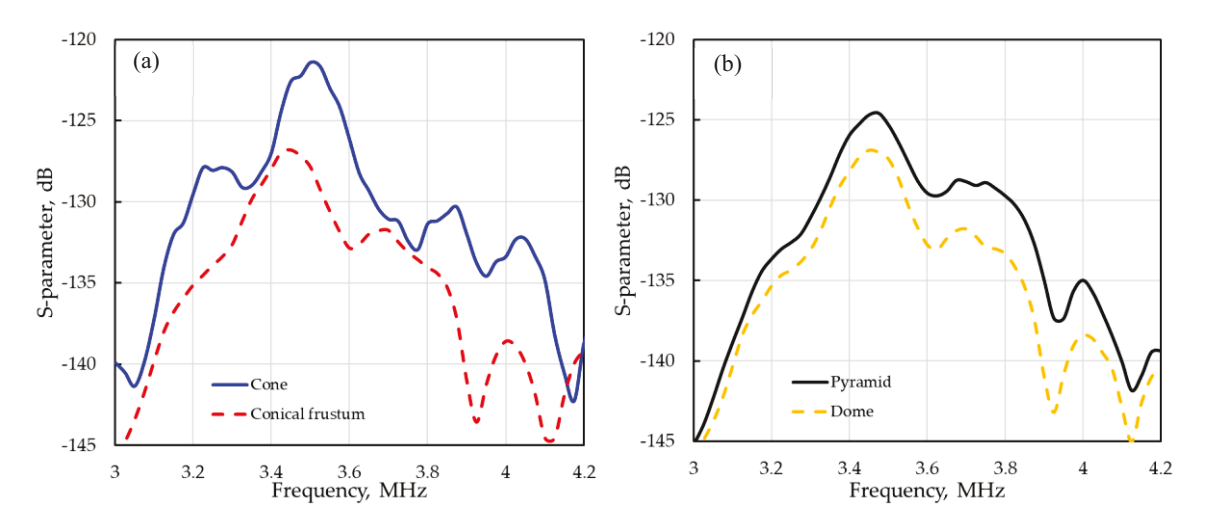


Figure 2. Scattering parameter (S_{21} in dB) as a function of frequency for different micro-shapes (a) cone/ conical frustum and (b) pyramid and dome.

2.3 Time domain study

A time domain analysis is studied to evaluate the change in input signal over time after adding microstructures in the sensing layer where the acoustic wave propagates. A transient analysis with an input sinusoidal response having 1V lasting 22 cycles at the resonant frequency is executed.

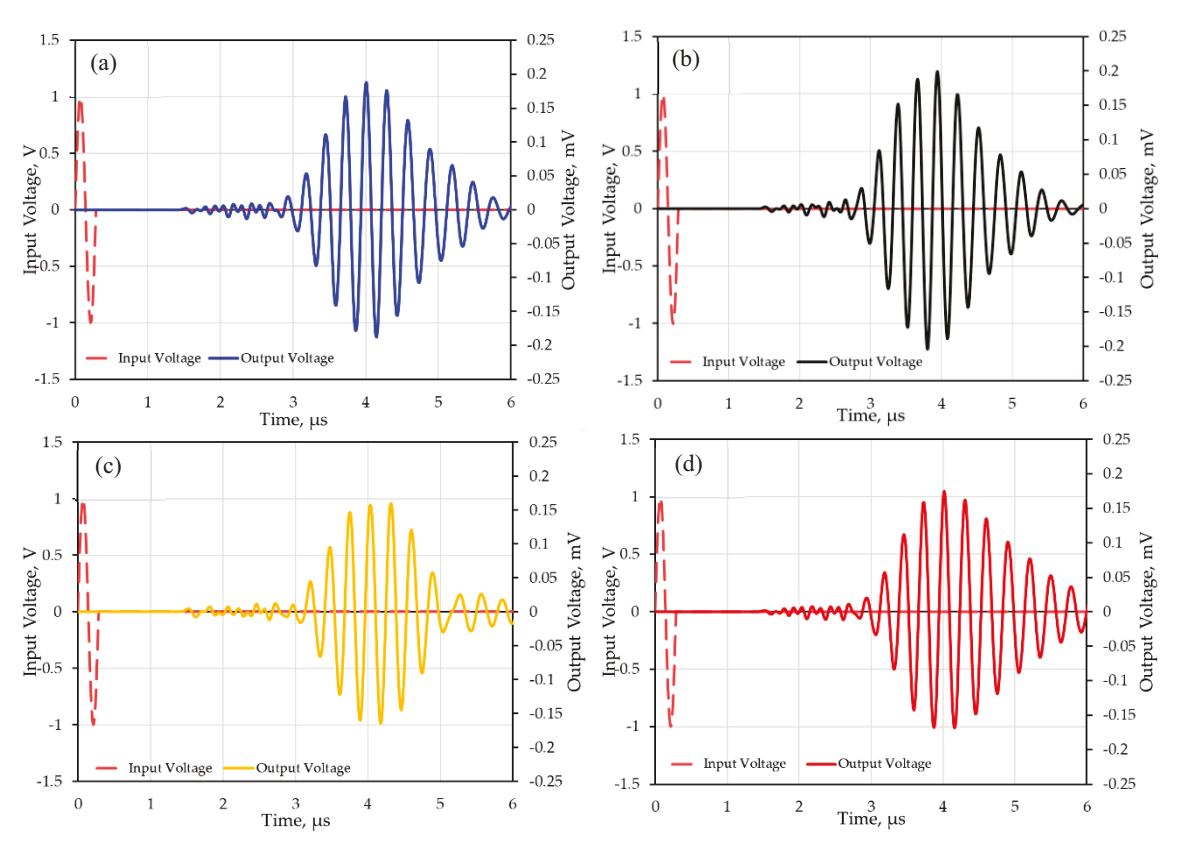


Figure 3. Voltage response as a function of time for different micro-shapes (a) cone; (b) pyramid; (c) dome, and (d) conical frustum.

The voltage amplitude is obtained from the output electrode, which converts the received mechanical wave into a voltage response, as shown in Figure 3 (a-d). Simulated results of the SAW sensor with microstructures are summarized in Table 3. Based on the numerical results, a 5-10% degradation of sensor response is noticed, in which the pyramid and cone exhibit better performance with an increase in surface area, which supports the microstructure concept. Sensors with pyramid and cone shaped microstructure grids are fabricated, and the response is validated with experimental results.

Table 3. Summary of sensor's frequency and time-domain analysis response with different microstructure shapes.

Micro-shapes	Frequency peak (MHz)	IL (dB)	Time delay (μs)	Output Signal (mV)
Conventional*	3.5	-120.16	3.68	0.228
Cone	3.5	-121.41	3.72	0.188
Pyramid	3.475	-124.58	3.71	0.201
Dome	3.45	-126.90	3.75	0.164
Conical frustum	3.45	-126.81	3.74	0.175

^{*}Conventional type represents the sensor without microstructures in the sensing layer.

3. DEVELOPMENT OF SAW DEVICE WITH MICROSTRUCTURE

3.1 Microstructure printing using the 2PP process

The microstructures design made of high viscous negative photoresist (IP-S, Nanoscribe, Karlsruhe, Germany) is printed using a 2PP printer (Photonic Professional GT2, Nanoscribe GmBH, Karlsruhe, Germany) equipped with a 780 nm femtosecond laser. IP-S resin and a 0.8 numerical aperture (NA) lens are utilized to increase the voxel size with quicker microstructure modeling. The printing parameters used for IP-S microstructures are 1 µm slicing distance, 0.5 µm hatching distance, 100 mm/sec base scan speed, and 60% laser power. The base layer count is also increased to avoid the floating of printed parts detached from the print bed.

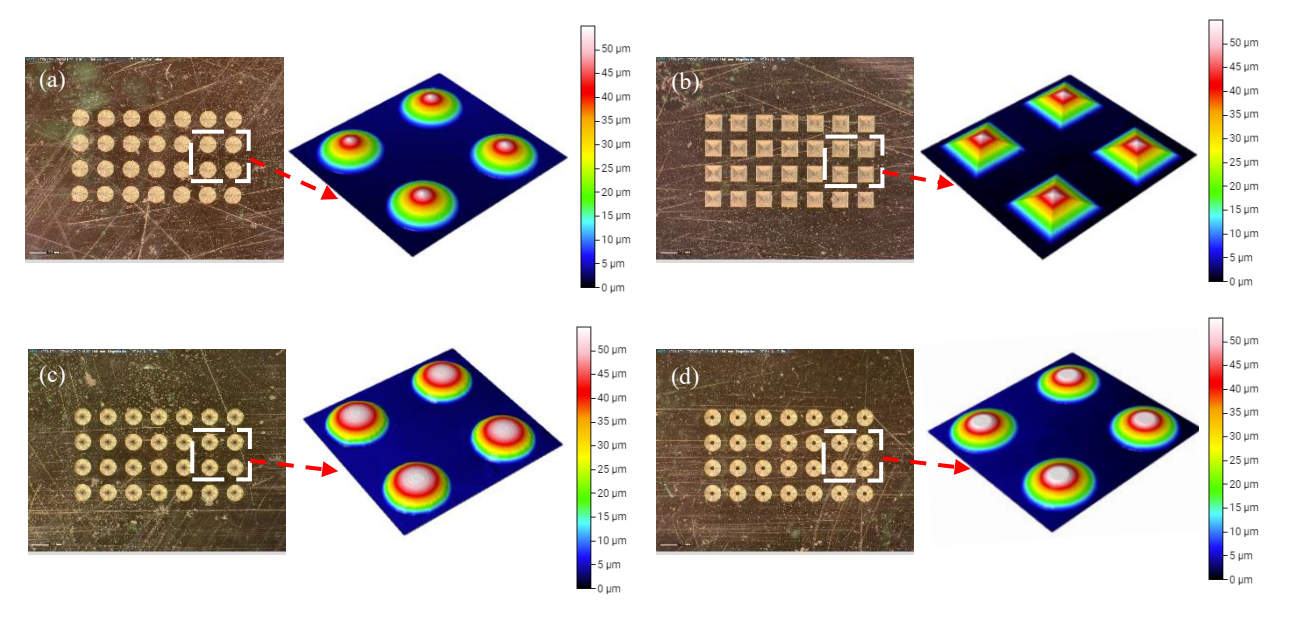


Figure 4. 2PP printed microstructures on PVDF film with scanned profiles (a) Cone; (b) Pyramid; (c) Dome, and (d) conical frustum.

To increase the adhesion between the microstructure and the PVDF film, the film is salinized, rendering the substrate surface hydrophobic and leading to a chemical bond between polymerized 2PP IP-S resin and substrate. The salinization process includes submerging the PVDF film in a mix of 15 mL acetone with 75 μ L of 3-(trimethoxysilyl)propyl methacrylate for 1~2 hours and washed with acetone followed by a deionized water rinse and blow-dried. To validate the printed microstructures' resolution, the printed parts are examined using a Filmetrics 3D profilometer with a spatial sampling of 0.176 μ m. For better conductivity, samples are sputtered with gold, and images are captured using a 50x objective with a 10 μ m and 70 μ m back scan and scan length, respectively, as shown in Figure 4.

3.2 Piezoelectric and mechanical properties of PVDF film

Piezoelectric properties are essential attributes that dictate a material's efficiency for sensing the targeted measurement. Material properties, such as piezoelectric strain coefficient (d), dielectric constant (ε), and piezoelectric voltage constant (g), are involved in the constitutive equation. The piezoelectric strain coefficient (d₃₃) is measured in the thickness direction using a YE2730 A piezometer. Permittivity is an essential property that enables the substrate to hold a charge for an extended period and is calculated using the standard parallel plate equation. The measured and calculated piezoelectric properties of the PVDF film are listed in Figure 5. From Figure 5, it can be noticed that permittivity decreases with an increase in frequency due to polarization drop. PVDF material's modulus, hardness, and dynamic viscoelastic properties, such as young's modulus (E), storage (E'), loss modulus (E''), and loss factor, are measured at a load of 5mN using a Hysitron TI-980 Tribo Indenter equipped with 100 nm radius Berkovich diamond indenter probe.

Material	t (µm)	d ₃₃ (pC/N)	εr	g ₃₃ (mVm/N)
PVDF	56	25.8	11	265

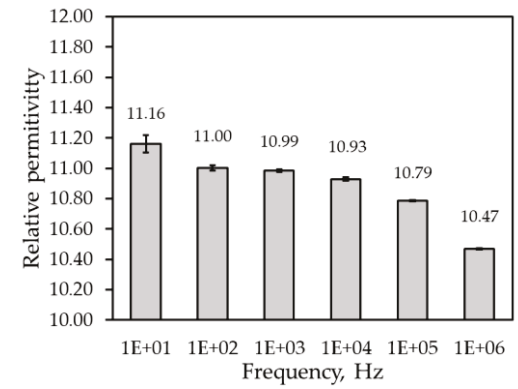


Figure 5. Piezoelectric and dielectric properties of PVDF film and frequency-dependent dielectric constant.

Figure 6 (a) indicates the measured reduced modulus of 2.18 ± 0.06 GPa, which is converted to young's modulus of 1.95 ± 0.06 GPa using Poisson's ratio of 0.3 and a hardness of 229.69 ± 10.32 MPa. Figure 6 (b) indicates the viscoelastic behavior of PVDF film under a frequency sweep from 10 Hz to 220 Hz, indicating storage modulus fluctuating within the deviation range with varying frequency and respective loss modulus and factor.

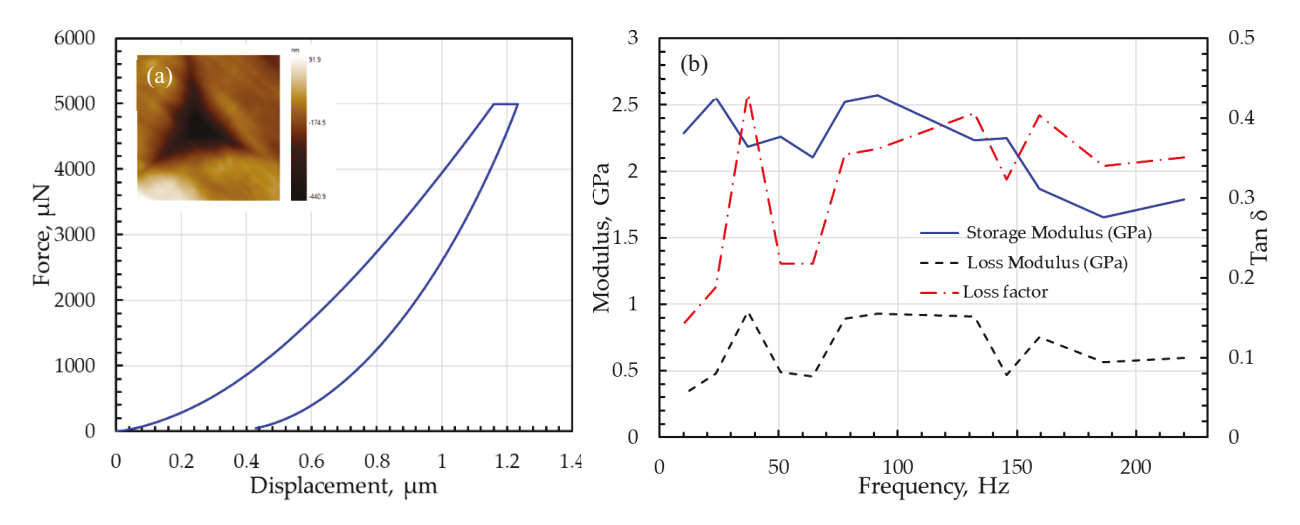


Figure 6. (a) Force vs. displacement curve of PVDF film tested with Berkovich tip impression and (b) nanoDMA frequency sweep demonstrating modulus and loss factor.

3.3 IDT Electrodes deposition

Gold sputter coater is used to deposit the conductive gold electrode under a vacuum by utilizing a stencil placed on top of the substrate covering the area of printed microstructures. The stencil with IDT pattern is designed and printed using a 2PP printer made of IP-Q resin equipped with a 0.3 numerical aperture (NA) lens, which acts as a mask between the sputter target and PVDF film, as shown in Figure 7 (a). The printing parameters used for the IP-Q stencil are 5 µm slicing distance, 1 µm hatching distance, 100 mm/sec base scan speed, and 90% laser power. Based on the numerical results, IDTs are deposited only on the film with pyramid and cone shape microstructures. Figure 7 (b) and (c) show well-bonded deposited IDT patterns without any discontinuity using the stencil and microstructures placed between them. A slight shadow effect near the microstructures is also noticed that can be avoided when depositing metal oxide thin film coated using feasible sputtering techniques.



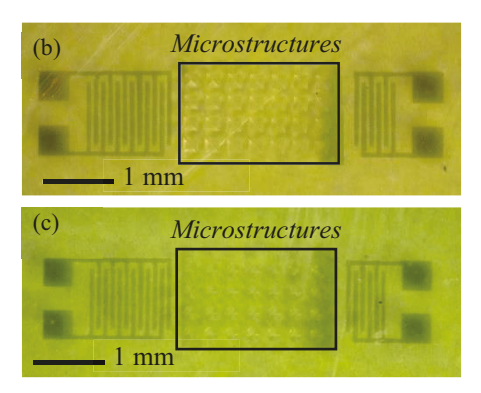
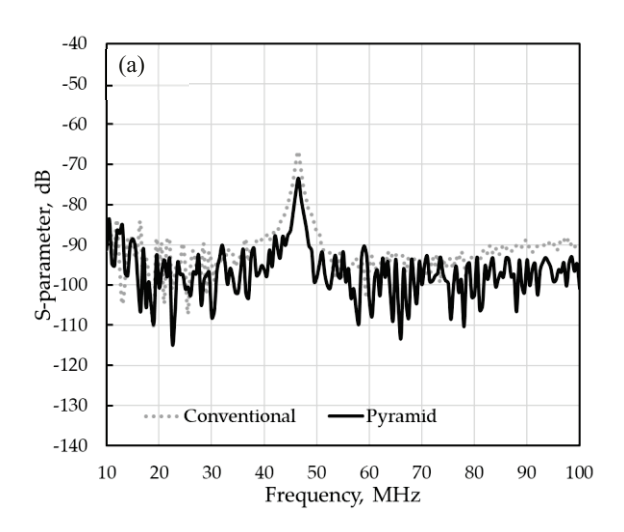


Figure 7. (a) 2PP printed stencil after sputtering; Sensor sputtered with gold electrodes (b) pyramid and (c) cone microstructure.

4. S-PARAMETER PERFORMANCE OF DEVELOPED SENSOR

The frequency response of the developed sensor with micro-structures (pyramid and cone) is measured using a network analyzer (N5227B) and two (40A-GSG-600-DP) pico-probes. The probes are calibrated using a CS-9 substrate, and a 10 dBm signal is given as an input with 50 Ω reference impedance.



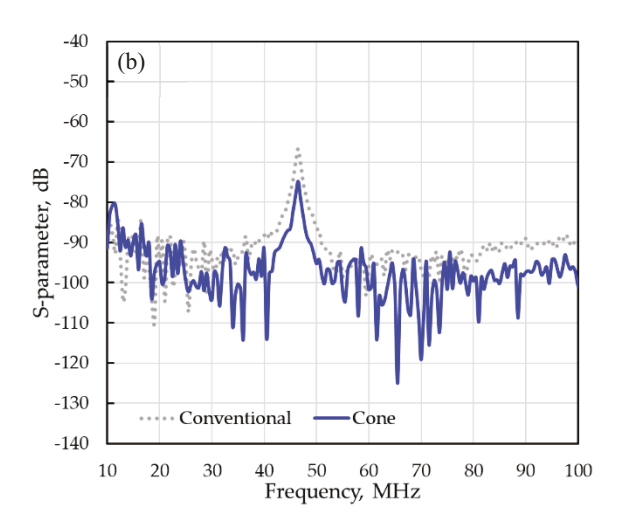


Figure 8. S-parameter VNA response of sensor with and without micro-structure (conventional) (a) pyramid and (b) cone.

The sensor response is measured in the frequency range from 10 MHz to 100 MHz providing frequency information, as shown in Figure 8 (a) and (b). The results reveal that there is no change in resonant frequency with the addition of microstructures to the sensing layer and a \sim 10% increase in insertion loss from -66.62 dB to -74.85 dB (cone) and -73.43 dB (pyramid), which supports the microstructures implementation. In summary, the wave characteristics didn't change or degrade upon including micro-structures into the sensor's sensing layer, which expands the application range by adding more sensing surface area. A harmonic resonant peak at 46.5 MHz is detected due to the ground probe interference with the piezoelectric substrate, which needs further investigation.

5. CONCLUSION

In summary, a piezoelectric sensor based on PVDF with electrodes and microstructures deposited on the surface is successfully developed through a novel 2PP high-resolution printer. The effect of adding different microstructure shapes in the sensing layer is numerically studied in both frequency and time domains. Pyramid and cone shapes are selected as ideal candidates for the gas sensing layer based on the numerical response. Sensor response with added microstructures is tested using VNA with RF probe setup and the result shows no change in sensor resonant peak, which significantly supports

the microstructure concept. In the future, microstructures will be coated with ZnO thin film through a suitable sputtering technique and tested under a targeted gas environment for effective sensing.

ACKNOWLEDGMENT

This material is based upon work supported by the National Science Foundation under Grants No. 2018853 and No. 2229155. The opinions, findings, and conclusions, or recommendations expressed are those of the author(s) and do not necessarily reflect the views of the National Science Foundation.

REFERENCES

- [1] Goswami, P., and Gupta, G., "Recent progress of flexible NO2 and NH3 gas sensors based on transition metal dichalcogenides for room temperature sensing," Materials Today Chemistry, 23, 100726 (2022).
- [2] Nikolic, M. V., Milovanovic, V., Vasiljevic, Z. Z. *et al.*, "Semiconductor gas sensors: Materials, technology, design, and application," Sensors, 20(22), 6694 (2020).
- [3] Nicolay, P., Chambon, H., Bruckner, G. et al., "A LN/Si-Based SAW Pressure Sensor," Sensors, 18(10), 3482 (2018).
- [4] Srinivasaraghavan Govindarajan, R., Rojas-Nastrucci, E., and Kim, D., "Surface Acoustic Wave-Based Flexible Piezocomposite Strain Sensor," Crystals, 11(12), 1576 (2021).
- [5] Xu, H., Dong, S., Xuan, W. *et al.*, "Flexible surface acoustic wave strain sensor based on single crystalline LiNbO3 thin film," Applied Physics Letters, 112(9), 093502 (2018).
- [6] Zhou, X., Tan, Q., Liang, X. *et al.*, "Novel multilayer SAW temperature sensor for ultra-high temperature environments," Micromachines, 12(6), 643 (2021).
- [7] Devkota, J., Ohodnicki, P. R., and Greve, D. W., "SAW sensors for chemical vapors and gases," Sensors, 17(4), 801 (2017).
- [8] Panneerselvam, G., Thirumal, V., and Pandya, H. M., "Review of surface acoustic wave sensors for the detection and identification of toxic environmental gases/vapours," Archives of Acoustics, 43(3), 357-367 (2018).
- [9] Patial, P., and Deshwal, M., "Systematic review on design and development of efficient semiconductor based surface acoustic wave gas sensor," Transactions on Electrical and Electronic Materials, 22(4), 385-393 (2021).
- [10] Ding, J., Chen, S., Han, N. *et al.*, "Aerosol assisted chemical vapour deposition of nanostructured ZnO thin films for NO2 and ethanol monitoring," Ceramics International, 46(10), 15152-15158 (2020).
- [11] Hasan, M. N., Maity, S., Sarkar, A. *et al.*, "Simulation and fabrication of SAW-based gas sensor with modified surface state of active layer and electrode orientation for enhanced H2 gas sensing," Journal of Electronic Materials, 46(2), 679 (2017).
- [12] Kang, Y., Yu, F., Zhang, L. et al., "Review of ZnO-based nanomaterials in gas sensors," Solid State Ionics, 360, 115544 (2021).
- [13] Waikar, M. R., Raste, P. M., Sonker, R. K. *et al.*, "Enhancement in NH3 sensing performance of ZnO thin-film via gamma-irradiation," Journal of Alloys and Compounds, 830, 154641 (2020).
- [14] Mourzina, Y., Steffen, A., and Offenhäusser, A., "The evaporated metal masks for chemical glass etching for BioMEMS," Microsystem technologies, 11(2-3), 135-140 (2005).
- [15] Rabeel, M., Javed, S., Khan, R. *et al.*, "Controlling the wettability of ZnO thin films by spray pyrolysis for photocatalytic applications," Materials, 15(9), 3364 (2022).
- [16] Srinivasaraghavan Govindarajan, R., Stark, T., Sikulskyi, S. *et al.*, [Piezoelectric strain sensor through reverse replication based on two-photon polymerization], SPIE, SS (2022).
- [17] Pérez, M., Carou, D., Rubio, E. M. et al., "Current advances in additive manufacturing," Procedia Cirp, 88, 439-444 (2020).
- [18] Srinivasaraghavan Govindarajan, R., Xu, X., Sikulskyi, S. *et al.*, "Additive manufacturing of flexible nanocomposite SAW sensor for strain detection," Sensors and Smart Structures Technologies for Civil, Mechanical, and Aerospace Systems 2021. 11591, 115910F.
- [19] Srinivasaraghavan Govindarajan, R., Madiyar, F., and Kim, D., "Flexible Piezoelectric Wave-Based Sensor: Numerical Analysis And Validation," Smart Materials, Adaptive Structures and Intelligent Systems. 86274, V001T05A007.